Langley

Copy
RM E57F25

CONFIDENTIAL

UNCLASSIFIED
CLASSIFICATION CHANGED
TO [illegible]
By authority of IPA #39 Date June 12, 1958
XRJ-GE

NACA RM E57F25

RESEARCH MEMORANDUM

PRELIMINARY INTERNAL PERFORMANCE DATA FOR A VARIABLE-EJECTOR ASSEMBLY ON THE XJ79-GE-1 TURBOJET ENGINE

II - AFTERBURNING CONFIGURATIONS

LIBRARY COPY
JUL 30 1957
LANGLEY AERONAUTICAL LABORATORY
LIBRARY, NACA
LANGLEY FIELD, VIRGINIA

By Harry E. Bloomer and Donald E. Groesbeck

Lewis Flight Propulsion Laboratory
Cleveland, Ohio

SPECIAL RELEASE
Restriction/Classification Cancelled
not given approval

FOR REFERENCE
NOT TO BE TAKEN FROM THIS ROOM

CLASSIFIED DOCUMENT
This material contains information affecting the national defense of the United States within the meaning of the espionage laws, Title 18, U.S.C., Sections 793 and 794. Its transmission or the revelation of its contents in any manner to unauthorized persons is prohibited by law.
Restriction/Classification Cancelled

NATIONAL ADVISORY COMMITTEE
FOR AERONAUTICS
WASHINGTON

CONFIDENTIAL

UNCLASSIFIED

CONFIDENTIAL

NATIONAL ADVISORY COMMITTEE FOR AERONAUTICS

RESEARCH MEMORANDUM

PRELIMINARY INTERNAL PERFORMANCE DATA FOR A VARIABLE-EJECTOR ASSEMBLY ON THE XJ79-GE-1 TURBOJET ENGINE

II - AFTERBURNING CONFIGURATIONS

By Harry E. Bloomer and Donald E. Groesbeck

4630

CX-1

SUMMARY

Internal performance of an XJ79-GE-1 variable ejector was experimentally determined with the primary nozzle in two representative afterburning positions. Jet-thrust and air-handling data were obtained in quiescent air for 4 selected ejector configurations over a wide range of secondary to primary airflow ratios and primary-nozzle pressure ratios. The experimental ejector data are presented in both graphical and tabulated form.

INTRODUCTION

The experimental performance of the XJ79-GE-1 variable-ejector assembly was investigated in an NACA Lewis altitude test chamber. The ejector assembly utilized independent control of the ejector-nozzle diameter, the primary exhaust-nozzle diameter, and the spacing between the two nozzles. In this investigation, the internal ejector performance was determined over a range of ejector geometry and operating conditions with the variable primary nozzle in two representative afterburning positions. Data for nonafterburning configurations are reported in reference 1.

Jet-thrust and air-handling data were obtained over a range of ejector operating conditions for each of 4 selected ejector configurations. Ejector diameter ratios of 1.21 and 1.37 were investigated for a primary exhaust-nozzle diameter of 27 inches and a spacing ratio of 0.78. For a primary-nozzle diameter of 29.25 inches and a spacing ratio of 0.71, ejector diameter ratios of 1.18 and 1.25 were investigated. Primary pressure ratio was varied from 2 to 11, and weight-flow ratio ranged from 0.035 to 0.28. Primary exhaust-gas temperature was approximately 2900° R (2440° F) for the 27-inch primary diameter and 3600° R (3140° F) for the 29.25-inch primary diameter. The secondary air was supplied at 500° R (40° F) for most of the data. During the investigation of one configuration, the secondary air was also supplied at 705° R (245° F) to simulate an engine-inlet flight condition of Mach 2.0 for a series of five data points.

CONFIDENTIAL

Conventional internal performance maps of jet-thrust ratios and total-pressure ratio are presented herein for the 4 ejector configurations investigated. In addition, all ejector data from the investigation are presented in tabulated form.

APPARATUS

Installation

The XJ79-GE-1 ejector installation in the altitude test chamber is shown photographically in figure 1 and schematically in figure 2. The forward bulkhead, which incorporates a labyrinth seal around the engine-inlet air duct, was used to separate the engine-inlet air from the exhaust and to provide a means of maintaining a pressure difference across the engine. A bulkhead butterfly valve was used to ventilate the test chamber. In this investigation, the engine was used as a gas generator for the ejector and was operated at rated conditions. Secondary air entered the test setup at an angle of 90° to the engine axis, so as not to impose an extraneous axial force. The entire assembly was mounted on a bedplate supported by flexure plates, as indicated in figure 2. Jet thrust was obtained from a calibrated null-type thrust cell after accounting for forces due to a pressure differential acting across the front bulkhead labyrinth-seal area. The over-all thrust-system accuracy was better than the system used in reference 1 and is believed to be accurate to within $\pm 1/2$ percent for the operating conditions of this investigation.

4630

Ejector System

The variable-geometry ejector assembly is schematically represented in figure 3. Separate sets of actuators permitted independent control of the primary-nozzle diameter, secondary-nozzle diameter, and axial spacing between the two nozzles. These dimensions were transmitted to the control room by a calibrated electromechanical system with an accuracy of ± 0.15 inch. Secondary air entered the plenum chamber from a single 8-inch pipe, and a sheet-metal baffle served to equalize the flow around the ejector annulus. A photograph is shown of the primary nozzle in figure 4 and of the ejector shroud in figure 5.

INSTRUMENTATION

Basic ejector instrumentation is indicated in figure 6. Primary-stream values of total pressure P_p were computed as arithmetic averages, since the probes were located in equal annular flow areas. (Symbols are defined in appendix A.) An arithmetic average was also used for the total pressure P_s and for the total temperature T_s of the secondary

stream because essentially no radial and circumferential profiles occurred at station s except at very low secondary airflows. Engine airflow and secondary airflow were determined from conventional pressure and temperature surveys indicated in figure 2. Secondary airflow was taken as that entering the plenum chamber, since very little leakage was found to occur between the plenum and station s. Ambient exhaust pressure was measured by 4 trailing static probes equally spaced around and 1 inch away from the ejector exit.

4630

CX-1 Back

PROCEDURE

Throughout most of the investigation, the engine was operated at a speed of about 7460 rpm, an inlet pressure of 1145 pounds per square foot absolute, and an inlet temperature of 500° R (40° F). The primary nozzle was held at either 27 or 29.25 inches in diameter, and the afterburner was operated to produce a turbine-outlet temperature of approximately 1540° R (1080° F). This resulted in primary temperature levels of approximately 2900° R (2440° F) and 3600° R (3140° F), respectively, and a primary gas flow of approximately 92 pounds per second. For one configuration, the engine-inlet conditions were changed to simulate a flight condition of Mach 2.0, the engine speed was raised to 7700 rpm, and the turbine-outlet temperature remained at 1540° R (1080° F).

Ejector weight-flow ratios were set by changing only the secondary flow, which was supplied at a constant temperature of 500° R (40° F) for most of the data. For the one configuration that was investigated at conditions simulating Mach 2.0, secondary air was also supplied at 705° R (245° F). Secondary flow was maintained almost constant for a desired number of data points by operating so as to choke both the secondary labyrinth-seal leakage and a supply valve upstream of the labyrinth seal. Primary pressure ratio was varied by changing only the ambient exhaust pressure.

Data for conventional performance maps were obtained by first setting a specific ejector geometry and then operating over a range of primary pressure ratios (2 to about 11) at several constant weight-flow ratios (0.035 to about 0.28). The 4 ejector configurations investigated in this manner are listed in table I, along with the range of operation for each. The primary gas temperature and nozzle coefficients were calculated as described in appendix B.

RESULTS

Performance maps of the 4 ejector configurations investigated are given in figures 7-10, and tabulated data are given in table II. Both jet-thrust ratio F_{ej}/F_{ip} and jet-thrust coefficient $F_{ej}/F_{ip} + F_{is}$

are presented in graphical form. The jet-thrust ratio is given because it is the conventional form used by aircraft manufacturers to obtain ejector thrust from engine performance; the jet-thrust coefficient is given because it is a measure of the isentropic efficiency of the ejector system. The performance maps exhibit typical ejector characteristics.

Jet-thrust ratio F_{ej}/F_{ip} peaked within the range of primary pressure ratios investigated for all configurations except number 2 (fig. 8), which had a large diameter ratio (1.37). For this configuration, the combined flow was not fully expanded with respect to ambient pressure within the range of primary pressure ratios investigated.

4630

Since few data points were obtained between primary pressure ratios of 2.25 and 4.0, the thrust coefficient curves are dashed in this region. However, it is expected that minimum jet-thrust ratios would occur in this region because of internal overexpansion losses.

The pumping curves for each ejector configuration indicate the usual "choking" of the secondary stream within the ejector at high primary pressure ratios. "Choking" means essentially that the secondary stream has been accelerated to its sonic velocity, and thus its total pressure (at station s) is no longer influenced by downstream conditions. This condition is indicated when the pumping curves become independent of primary pressure ratio, that is, when secondary pressure ratio becomes constant with increasing primary pressure ratio.

Since only 4 configurations were evaluated, no attempt has been made in this report to find the optimum diameter ratio as in reference 1. In general, however, the thrust coefficients for configuration 3 show the highest performance level ($D_s/D_p = 1.25$). Configuration 2 ($D_s/D_p = 1.37$) is probably beyond the optimum diameter ratio for highest performance.

Temperature rise for the secondary air shown in figure 11 can be used to evaluate ejector temperature ratio for all 4 ejector configurations. (When the cooling air is supplied at 705° R, the data separate widely from the 500° R curves. By plotting temperature rise against corrected flow ratio $W_s/W_p\sqrt{T_s/T_p}$, the data may be generalized.) The data from reference 1 at a primary temperature of 1410° R is shown for comparative purposes.

The effect of weight-flow ratio on the mass distribution around the shroud is presented in figure 12. At high secondary flow, the distribution was quite uniform. As the secondary weight flow decreased to 0.033, the variation in flow distribution increased to a spread of 16.5 points between the circumferential locations of 90° and 180°.

APPLICATION OF DATA

All data contained in this report apply directly to only the specific ejector configurations operating at specific primary and secondary temperatures. However, the data can be interpolated for systematic variations in geometry, weight-flow ratio, and pressure ratio.

To apply these data to the same ejector system operating at other primary or secondary temperatures, the conventional corrected weight-flow parameter $W_s/W_p\sqrt{T_s/T_p}$ should be used.

The assumptions involved in this method are:

$$\left(\frac{W_s}{W_p}\sqrt{\frac{T_s}{T_p}}\right)_{test} = \left(\frac{W_s}{W_p}\sqrt{\frac{T_s}{T_p}}\right)_{flight}$$

and

$$\left(\frac{F_{ej}}{F_{ip}}\right)_{test} = \left(\frac{F_{ej}}{F_{ip}}\right)_{flight}$$

(For extrapolations of data below a primary temperature of 1700° R, use ref. 1.)

The data do not include any effect of base drag or of free stream on internal ejector performance. Ejector base drag is influenced by the fuselage or nacelle configuration preceding an ejector installation. The free-stream effect should be negligible when the ejector is operated at "choking" conditions.

Lewis Flight Propulsion Laboratory
National Advisory Committee for Aeronautics
Cleveland, Ohio, June 26, 1957

4630

APPENDIX A

SYMBOLS

A_{eff} effective flow area $A_p \times \frac{W_p}{(W_p)_{cr}}$, sq ft

A_p measured flow area of primary nozzle, sq ft

C_D flow coefficient for primary nozzle, $C_D = \frac{W_p}{(W_p)_{cr}} = \frac{A_{eff}}{A_p}$

D_e measured diameter of ejector exit, in.

D_p measured diameter of primary-nozzle exit, in.

F_{ej} measured jet thrust of ejector system, lb

F_{ip} jet thrust ideally available from complete isentropic expansion of primary flow, $\left(\frac{W_p}{g}\right) V_{ip}$, lb

F_{is} jet thrust ideally available from complete isentropic expansion of secondary flow, $\left(\frac{W_s}{g}\right) V_{is}$, lb

g acceleration due to gravity, 32.17 ft/sec^2

L spacing, distance between primary- and secondary-nozzle exits, in.

P_p average total pressure of primary stream at station p, lb/sq ft abs

P_s average total pressure of secondary stream at station s, lb/sq ft abs

p_o ambient exhaust pressure, lb/sq ft abs

R universal gas constant

T_c total temperature of secondary air entering plenum chamber, ^oR

T_p average total temperature of primary stream at station p, ^oR

T_s average total temperature of secondary stream at station s, ^oR

4630

V_{eff} effective velocity of ideal convergent nozzle, ft/sec

V_{ip} ideal velocity of complete isentropic expansion from P_p and T_p to p_0, ft/sec

V_{is} ideal velocity of complete isentropic expansion from P_s and T_s to p_0, ft/sec

W_p measured primary gas flow, lb/sec

$(W_p)_{cr}$ critical one-dimensional primary flow, computed from A_p, P_p, T_p, and γ_p, lb/sec

W_s measured secondary airflow, lb/sec

α_p half-cone angle of primary nozzle, $\sin^{-1}\left(1.79 - \frac{D_p}{17.2}\right) - 3$, deg

α_s half-cone angle of ejector shroud, $\sin^{-1}\left(1.29 - \frac{D_s}{26.8}\right) + 5$, deg

γ_p ratio of specific heats for primary stream, 1.28

4630

APPENDIX B

CALCULATION OF PRIMARY GAS TEMPERATURE AND NOZZLE COEFFICIENTS

The following diagram represents the engine-ejector installation:

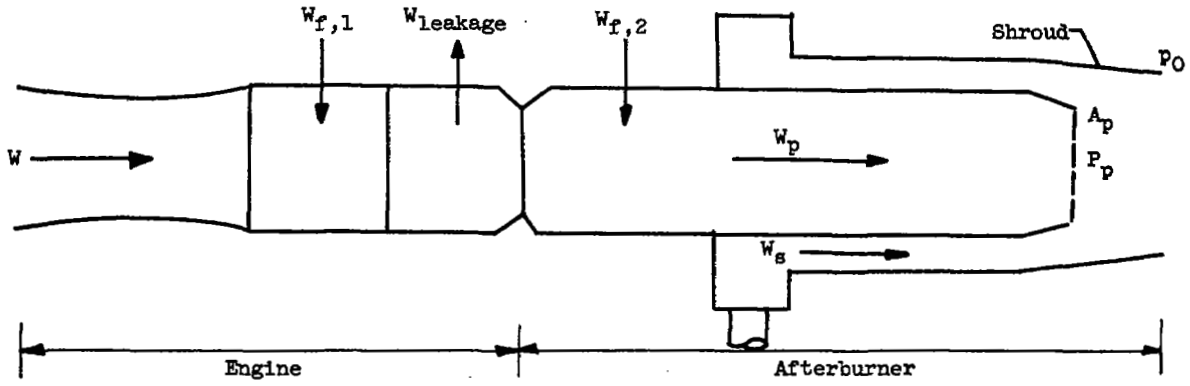

The primary mass flow W_p was the sum of engine airflow W plus engine fuel flow $W_{f,1}$ plus afterburner fuel flow $W_{f,2}$ minus leakage flow $W_{leakage}$. Primary gas temperature was calculated from total pressure taken at station p P_p, ambient pressure p_0, primary nozzle area A_p, and a primary nozzle flow coefficient determined from previous data $C_D = 0.99$.

$$T_p = \left[\frac{C_D A_p \left(1.25\, P_p - p_0\right)}{\sqrt{\frac{R}{g}}\, W_p \, \frac{V_{eff}}{\sqrt{gRT_p}}} \right]$$

where $\frac{V_{eff}}{\sqrt{gRT_p}}$ is an effective velocity parameter which is a function of $\frac{p_0}{P_p}$ (ref. 2), and $1.25 = (\gamma + 1)\left(\frac{2}{\gamma + 1}\right)^{\frac{\gamma}{\gamma - 1}}$ when $\gamma = 1.27$. The ejector jet-thrust ratio $\frac{F_{ej}}{F_{ip}}$ was determined from the following relation:

$$\frac{F_{ej}}{F_{ip}} = \frac{\text{Measured jet thrust}}{\left(\frac{W_p}{g}\right) V_{ip}}$$

[redacted]

4630

where V_{ip} is determined by using an ideal velocity parameter (ref. 2) that is a function of p_0/P_p, and by using T_p to find an isentropic velocity of complete expansion to ambient pressure. The ejector jet-thrust coefficient $F_{ej}/F_{ip} + F_{is}$ was determined from the following relation:

$$\frac{F_{ej}}{F_{ip} + F_{is}} = \frac{\text{Measured jet thrust}}{\frac{W_p}{g} V_{ip} + \frac{W_s}{g} V_{is}}$$

where V_{ip} and V_{is} are isentropic velocities of complete expansion. In cases where P_s was less than p_0, F_{is} was assumed to be zero.

REFERENCES

1. Greathouse, William K., and Bloomer, Harry E.: Preliminary Internal Performance Data for a Variable-Ejector Assembly on the XJ79-GE-1 Turbojet Engine. I - Nonafterburning Configurations. NACA RM E56E23, 1956.

2. Turner, L. Richard, Addie, Albert N., and Zimmerman, Richard H.: Charts for the Analysis of One-Dimensional Steady Compressible Flow. NACA TN 1419, 1948.

4630

CX-2

TABLE I. - EJECTOR CONFIGURATIONS AND TEST CONDITIONS

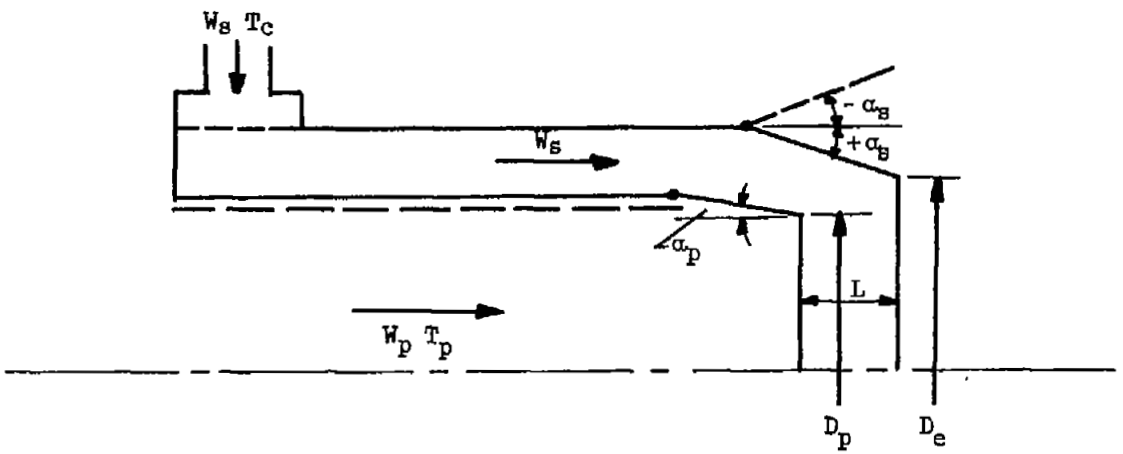

Ejector configuration	Primary diameter, D_p, in.	Diameter ratio, D_e/D_p	Spacing ratio, L/D_p	Secondary half-cone angle, α_s, deg	Primary half-cone angle, α_p, deg	Range of primary pressure ratio, P_p/p_0	Range of weight flow ratio, W_s/W_p	Data in figure
1	27.0	1.21	0.78	+3.56	11.70	2.25 - 10.8	0.030 - .124	7
2	27.0	1.37	.78	-5.62	11.70	2.25 - 11.0	.033 - .28	8
3	29.25	1.25	.71	-4.76	4.88	2.01 - 11.0	.060 - .24	9
4	29.25	1.18	.71	-0.34	4.88	2.18 - 10.0	.060 - .285	10

TABLE II. - NOMINAL EJECTOR GEOMETRY

(a) Configuration 1: Diameter ratio D_e/D_p, 1.21; spacing ratio L/D_p, 0.78; primary-nozzle-exit diameter D_p, 27.00 inches

Run	Ejector geometry		Performance parameters						Weight flow			Pressure			Temperature			Measured ejector jet thrust, F_{ej}, lb
	Spacing ratio, L/D_p	Diameter ratio, D_e/D_p	Ejector weight-flow ratio, W_s/W_p	Primary pressure ratio, P_p/P_0	Ejector total-pressure ratio, P_s/P_p	Ejector jet-thrust ratio, F_{ej}/F_{ip}	Ejector jet-thrust coefficient, $\frac{F_{ej}}{F_{ip}+F_{is}}$	Primary to secondary temperature ratio, T_p/T_s	$\frac{W_s}{W_p}\sqrt{\frac{T_s}{T_p}}$	Primary gas flow, W_p, lb/sec	Secondary air flow, W_s, lb/sec	Primary total pressure, P_p, lb/sq ft abs	Secondary total pressure, P_s, lb/sq ft abs	Ambient exhaust pressure, P_0, lb/sq ft abs	Primary total temperature, T_p, °R	Secondary total temperature, T_s, °R	Ejector supply air temperature, T_o, °R	
1	0.78	1.21	0.030	2.29	0.576	0.922	0.922	4.07	0.015	91.54	2.72	2473	929	1061	2961	733	501	7,501
2			.033	4.02	.252	.930	.930	3.78	.017	90.98	3.01	2451	568	610	2958	782	502	9,186
3			.037	5.91	.198	.946	.940	3.50	.020	91.12	3.40	2413	472	408	2852	815	502	10,185
4			.039	10.81	.183	.945	.934	3.96	.020	90.61	3.57	2412	442	223	2906	734	502	11,454
5			.083	2.26	.408	.950	.950	4.47	.030	91.57	5.76	2437	989	1078	2094	647	502	7,378
6			.088	4.00	.258	.939	.935	4.57	.032	91.77	6.34	2460	629	615	2945	645	502	9,318
7			.087	6.02	.231	.952	.949	4.54	.031	90.81	6.07	2419	558	402	2922	643	503	10,468
8			.089	10.62	.214	.983	.944	4.56	.032	90.51	6.25	2430	520	229	2948	646	503	11,715
9			.122	2.25	.437	.977	.977	5.05	.064	91.54	11.19	2448	1069	1085	2904	575	502	7,581
10			.124	3.89	.291	.973	.957	5.08	.065	91.32	11.32	2445	711	628	2917	574	503	9,490
11			.121	6.18	.264	.987	.960	5.04	.064	91.78	11.13	2448	547	398	2898	575	503	10,897
12			.120	10.24	.255	.985	.951	5.15	.063	90.70	10.91	2447	825	259	2966	576	503	11,971

(b) Configuration 2: Diameter ratio D_e/D_p, 1.37; spacing ratio L/D_p, 0.78; primary-nozzle-exit diameter D_p, 27.00 inches

Run	Ejector geometry		Performance parameters						Weight flow			Pressure			Temperature			Measured ejector jet thrust, F_{ej}, lb
	Spacing ratio, L/D_p	Diameter ratio, D_e/D_p	Ejector weight-flow ratio, W_s/W_p	Primary pressure ratio, P_p/P_0	Ejector total-pressure ratio, P_s/P_p	Ejector jet-thrust ratio, F_{ej}/F_{ip}	Ejector jet-thrust coefficient, $\frac{F_{ej}}{F_{ip}+F_{is}}$	Primary to secondary temperature ratio, T_p/T_s	$\frac{W_s}{W_p}\sqrt{\frac{T_s}{T_p}}$	Primary gas flow, W_p, lb/sec	Secondary air flow, W_s, lb/sec	Primary total pressure, P_p, lb/sq ft abs	Secondary total pressure, P_s, lb/sq ft abs	Ambient exhaust pressure, P_0, lb/sq ft abs	Primary total temperature, T_p, °R	Secondary total temperature, T_s, °R	Ejector supply air temperature, T_o, °R	
13	0.78	1.37	0.035	2.26	0.418	0.932	0.932	4.13	0.017	92.77	3.27	2480	1036	1099	2899	702	497	7,354
14			.033	4.11	.203	.901	.901	4.04	.017	91.99	3.07	2529	514	616	3091	766	497	9,263
15			.036	6.01	.168	.931	.929	3.75	.020	92.23	3.49	2487	418	414	2953	792	497	10,390
16			.036	11.00	.165	.950	.942	3.88	.018	91.18	3.24	2485	386	226	3016	777	498	11,879
17			.068	2.25	.427	.952	.952	4.28	.028	92.60	5.35	2443	1044	1086	2831	660	498	7,390
18			.066	2.33	.410	.935	.935	4.43	.026	90.93	5.05	2435	999	1044	2916	658	497	7,397
19			.058	3.91	.230	.936	.936	4.29	.028	92.42	5.32	2426	567	621	2805	654	496	9,090
20			.057	5.94	.190	.949	.942	4.28	.026	92.51	5.31	2433	462	410	2775	648	495	10,273
21			.060	10.31	.175	.965	.941	4.29	.029	91.28	5.46	2433	421	236	2891	674	495	11,591
22			.093	2.21	.444	.959	.959	4.80	.042	91.93	8.55	2435	1082	1101	2855	594	497	7,350
23			.088	3.96	.247	.942	.942	4.81	.040	91.93	8.13	2430	600	614	2846	592	497	9,215
24			.088	6.01	.204	.950	.937	4.82	.040	91.96	8.12	2433	497	406	2852	592	497	10,393
25			.092	9.88	.196	.965	.943	4.94	.042	90.85	8.38	2432	478	246	2922	591	497	11,629
26		1.58	----	2.20	.454	.965	.965	4.85	----	92.70	----	2473	1122	1125	2908	588	503	7,493
27			.111	3.98	.280	.960	.956	4.92	.050	92.27	10.27	2444	656	615	2864	582	499	9,454
28			.111	5.06	.222	.970	.950	4.90	.050	92.52	10.29	2450	545	404	2865	585	497	10,709
29			.106	9.75	.217	.984	.967	4.96	.047	91.91	9.71	2455	532	252	2904	588	496	11,909
30			.169	2.24	.480	.974	.964	5.19	.074	92.71	15.62	2463	1152	1099	2886	556	498	7,617
31			.166	4.05	.290	.989	.958	5.23	.073	92.23	15.34	2448	711	607	2879	551	496	9,706
32			.172	6.31	.263	.994	.958	5.17	.076	93.16	16.00	2459	646	390	2849	551	495	11,111
33			.171	9.21	.257	1.000	.957	5.31	.074	92.50	15.80	2467	535	268	2921	550	494	12,102
34			.275	2.25	.487	.988	.954	5.40	.119	92.80	25.55	2480	1207	1097	2950	543	501	7,805
35			.278	4.23	.347	.998	.945	5.45	.119	91.88	25.55	2487	856	583	2960	543	498	10,118
36			.276	6.99	.332	1.020	.948	5.28	.120	92.68	25.58	2447	815	350	2848	539	497	11,548
37			.281	8.68	.336	1.030	.945	5.39	.121	92.00	25.85	2448	822	282	2898	538	497	12,192

TABLE II. - Continued. NOMINAL EJECTOR GEOMETRY

(c) Configuration 3: Diameter ratio D_e/D_p, 1.25; spacing ratio L/D_p, 0.71; primary-nozzle-exit diameter D_p, 29.25 inches

Run	Ejector geometry		Performance parameters						Weight flow			Pressure			Temperature			Measured ejector jet thrust, F_{ej}, lb
	Spacing ratio, L/D_p	Diameter ratio, D_e/D_p	Ejector weight-flow ratio, W_s/W_p	Primary pressure ratio, P_p/P_0	Ejector total-pressure ratio, P_s/P_p	Ejector jet-thrust ratio, F_{ej}/F_{ip}	Ejector jet-thrust coefficient, $\frac{F_{ej}}{F_{ip} + F_{is}}$	Primary to secondary temperature ratio, T_p/T_s	$\frac{W_s}{W_p}\sqrt{\frac{T_s}{T_p}}$	Primary gas flow, W_p, lb/sec	Secondary air flow, W_s, lb/sec	Primary total pressure, P_p, lb/sq ft abs	Secondary total pressure, P_s, lb/sq ft abs	Ambient exhaust pressure, p_0, lb/sq ft abs	Primary total temperature, T_p, °R	Secondary total temperature, T_s, °R	Ejector supply air temperature, T_o, °R	
38	0.71	1.27	0.080	2.07	0.455	0.953	0.953	5.54	0.026	93.66	6.63	2378	1082	1148	3605	651	498	8,045
39		1.26	.065	3.89	.278	.957	.954	5.44	.028	92.88	6.03	2353	654	638	3596	661	498	10,389
40		1.26	.063	5.65	.252	.970	.957	5.23	.028	93.48	5.93	2349	592	416	3546	678	497	11,849
41		1.26	.061	9.63	.245	.974	.958	5.35	.026	92.23	5.59	2351	577	244	3678	688	500	13,262
42		1.25	.085	5.80	.257	.971	.958	5.73	.027	95.87	6.25	2406	618	415	3541	618	493	12,207
43		1.24	.067	5.92	.257	.969	.956	5.83	.029	95.69	6.40	2417	622	408	3596	617	493	12,327
44		1.27	.073	9.29	.256	.979	.960	5.78	.030	93.84	6.83	2394	613	258	3657	633	499	13,461
45		1.25	.074	10.98	.258	.975	.955	6.02	.030	95.00	7.04	2416	623	220	3659	608	495	13,914
46		1.26	.084	2.14	.449	.956	.956	5.82	.035	94.19	7.89	2370	1085	1108	3545	609	497	8,203
47		1.26	.082	3.88	.289	.963	.953	5.91	.034	93.17	7.62	2343	677	604	3549	601	497	10,581
48		1.26	.090	5.72	.271	.979	.960	5.82	.037	94.25	8.47	2357	659	412	3511	603	496	12,038
49		1.26	.089	9.27	.265	.985	.962	5.92	.036	92.75	8.21	2345	622	253	3587	606	496	13,274
50	.70	1.25	.133	2.17	.461	.969	.969	6.45	.053	94.55	12.61	2408	1109	1110	3864	568	498	8,543
51	.70	1.25	.137	3.94	.316	.974	.953	6.36	.054	94.84	12.99	2405	759	611	3649	574	497	11,071
52	.69	1.25	.138	6.01	.301	.991	.960	6.37	.055	94.50	13.03	2402	723	400	3688	576	497	12,602
53	.69	1.26	.139	10.34	.300	1.011	.975	6.52	.054	93.29	12.93	2399	720	234	3756	578	498	14,257
54	.72	1.22	.148	2.01	.504	.969	.965	6.37	.059	93.83	13.92	2381	1200	1183	3594	564	498	8,008
55	.71	1.25	.155	5.96	.329	1.016	.979	6.36	.061	93.98	14.55	2373	781	398	3569	561	499	12,650
56		1.26	.157	9.56	.333	1.016	.972	6.49	.062	93.23	14.62	2368	788	253	3642	561	502	13,859
57		1.25	.154	10.27	.334	1.017	.972	6.31	.061	91.04	14.02	2311	772	225	3636	576	517	13,731
58		1.22	.841	2.01	.536	1.001	.975	6.69	.093	94.19	22.73	2392	1287	1188	3632	543	486	8,354
59		1.26	.229	6.00	.399	1.040	.978	6.62	.089	94.27	21.60	2380	950	597	3617	546	496	13,071
60		1.25	.235	7.25	.404	(a)	(a)	6.58	.092	93.44	21.92	2355	951	325	3592	546	497	(a)
61		1.25	.235	8.46	.399	1.054	.986	6.64	.091	94.47	22.23	2386	953	282	3610	544	496	14,239
62	.70	1.23	.130	5.18	.318	.991	.959	5.82	.054	36.21	5.13	907	288	175	3524	606	494	4,567
63	.70	1.23	.084	5.31	.271	.970	.954	5.41	.036	36.58	3.06	913	247	172	3475	642	497	4,512
64	.69	1.27	.239	4.44	.390	1.018	.962	6.19	.096	36.85	8.79	920	359	207	3496	565	498	4,564
65	.70	1.23	.241	4.51	.395	1.022	.964	6.24	.096	36.23	8.72	907	358	201	3518	564	496	4,536
66[b]	.70	1.23	.139	9.63	.315	.989	.943	4.34	.067	109.38	15.21	2648	835	275	3309	763	691	15,157

[a] Cooling air on.

[b] Free-stream Mach number, 2.0.

TABLE II. - Concluded. NOMINAL EJECTOR GEOMETRY

(d) Configuration 4: Diameter ratio D_s/D_p, 1.18; spacing ratio L/D_p, 0.71; primary-nozzle-exit diameter D_p, 29.25 inches

Run	Ejector geometry		Performance parameters						Weight flow			Pressure			Temperature			Measured ejector jet thrust, F_{ej}, lb
	Spacing ratio, L/D_p	Diameter ratio, D_s/D_p	Ejector weight-flow ratio, W_s/W_p	Primary pressure ratio, P_p/P_0	Ejector total-pressure ratio, P_s/P_p	Ejector jet thrust ratio, F_{ej}/F_{ip}	Ejector jet-thrust coefficient, $\frac{F_{ej}}{F_{ip}+F_{is}}$	Primary to secondary temperature ratio, T_p/T_s	$\frac{W_s}{W_p}\sqrt{\frac{T_s}{T_p}}$	Primary gas flow, W_p, lb/sec	Secondary air flow, W_s, lb/sec	Primary total pressure, P_p, lb/sq ft abs	Secondary total pressure, P_s, lb/sq ft abs	Ambient exhaust pressure, P_0, lb/sq ft abs	Primary total temperature, T_p, °R	Secondary total temperature T_s, °R	Ejector supply air temperature, T_o, °R	
67	0.71	1.18	0.066	2.21	0.419	0.936	0.936	5.67	0.028	92.85	8.11	2590	1002	1084	3741	680	501	8,243
68	.71	1.18	.061	3.63	.277	.950	.945	5.54	.026	93.05	5.67	2584	660	822	3699	668	501	10,575
69	.69	1.20	.067	4.94	.253	.964	.953	5.53	.029	94.41	6.37	2580	602	482	3690	649	499	11,548
70	.71	1.18	.064	6.83	.255	.972	.958	5.29	.028	93.54	6.02	2565	602	599	3599	681	501	12,079
71	.71	1.18	.064	9.47	.248	.980	.962	5.36	.028	92.29	5.94	2548	585	248	3665	684	500	13,289
72	.69	1.20	.068	9.56	.245	.972	.955	5.52	.028	91.07	6.98	2524	564	243	3689	688	512	13,075
73	.71	1.18	.086	2.19	.445	.967	.967	5.86	.036	92.55	7.97	2544	1044	1086	3587	612	497	8,250
74			.087	3.62	.307	.972	.964	5.67	.036	92.86	8.10	2538	719	665	3572	609	503	10,326
75			.094	6.13	.277	.988	.987	5.88	.039	92.32	8.67	2528	646	380	3586	611	504	12,216
76			.099	10.01	.274	.987	.980	5.99	.040	91.72	9.04	2552	638	255	3657	610	499	13,411
77			.139	2.234	.457	.980	.975	6.34	.055	91.88	12.72	2550	1064	1043	3599	568	500	8,464
78			.157	4.20	.338	.991	.972	6.25	.065	93.78	12.82	2558	796	562	3545	567	499	11,303
79			.140	5.89	.332	1.01	.974	6.30	.055	93.48	13.06	2545	777	398	3541	562	496	12,426
80			.144	8.39	.327	-----	-----	6.30	.057	93.87	13.50	2585	775	282	3559	565	498	------
81			.181	2.16	.498	.981	.985	6.46	.071	92.50	16.72	2553	1167	1089	3619	560	503	8,387
82	.72		.188	3.91	.380	1.01	.971	6.40	.074	92.81	17.43	2570	900	806	3635	568	504	11,214
83			.187	6.18	.389	1.02	.970	6.31	.074	92.80	17.35	2563	875	582	3616	575	507	12,733
84			.184	8.80	.388	1.02	.988	6.40	.073	91.85	16.86	2551	861	267	3671	574	508	13,578
85			.282	2.14	.542	.998	.988	6.62	.109	92.16	25.95	2574	1287	1112	3699	559	504	8,534
86			.285	4.00	.454	1.03	.983	6.53	.112	92.73	26.44	2572	1076	693	3648	559	506	11,547
87			.284	6.50	.448	1.05	.970	6.51	.111	91.97	26.09	2559	1056	383	3664	563	507	13,242
88			.281	8.00	.451	1.05	.983	6.54	.110	91.77	25.79	2552	1061	294	3665	560	508	13,697
[b]89	.71	1.21	.067	7.21	.257	.980	.980	3.61	.036	58.71	3.96	1354	348	188	2985	829	699	7,267
[b]90	.71	1.21	.125	6.75	.315	1.01	.967	3.90	.063	58.82	7.29	1350	425	200	2991	788	705	7,342
[b]91	0	1.21	.190	6.47	.375	1.03	.968	4.09	.094	57.85	10.98	1353	507	209	3074	752	704	7,465
[b]92	.68	1.20	.066	3.67	.277	.963	.946	3.42	.036	52.27	2.13	727	201	188	2859	657	702	3,245
[b]93	0	1.20	.126	3.65	.325	.992	.969	3.67	.066	52.22	4.05	737	240	202	2936	800	705	3,358

[b]Free-stream Mach number, 2.0.

(a) Side view.

Figure 1. - XJ79-GE-1 engine ejector installation.

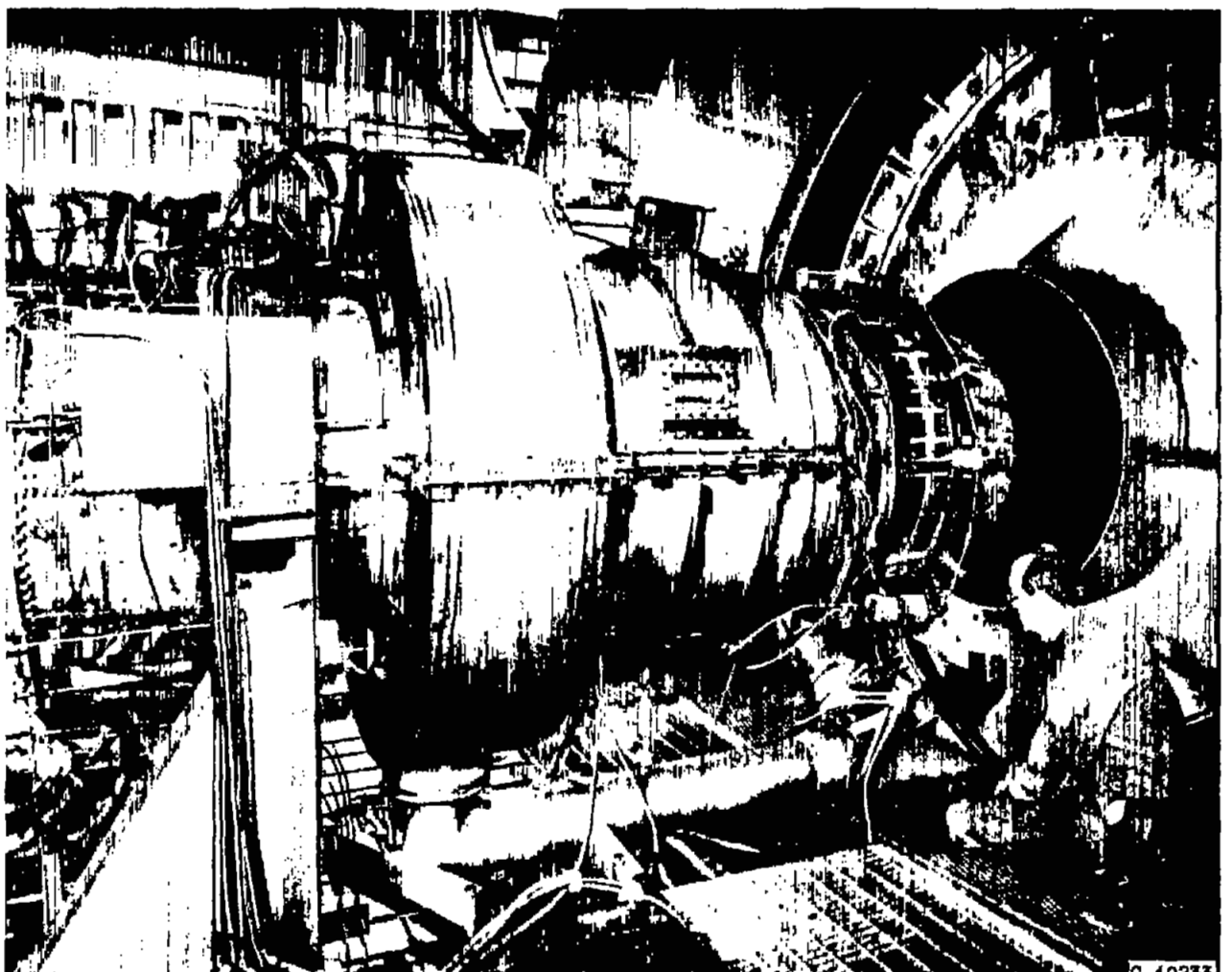

(b) Three-quarter view.

Figure 1. - Concluded. XJ79-GE-1 engine ejector installation.

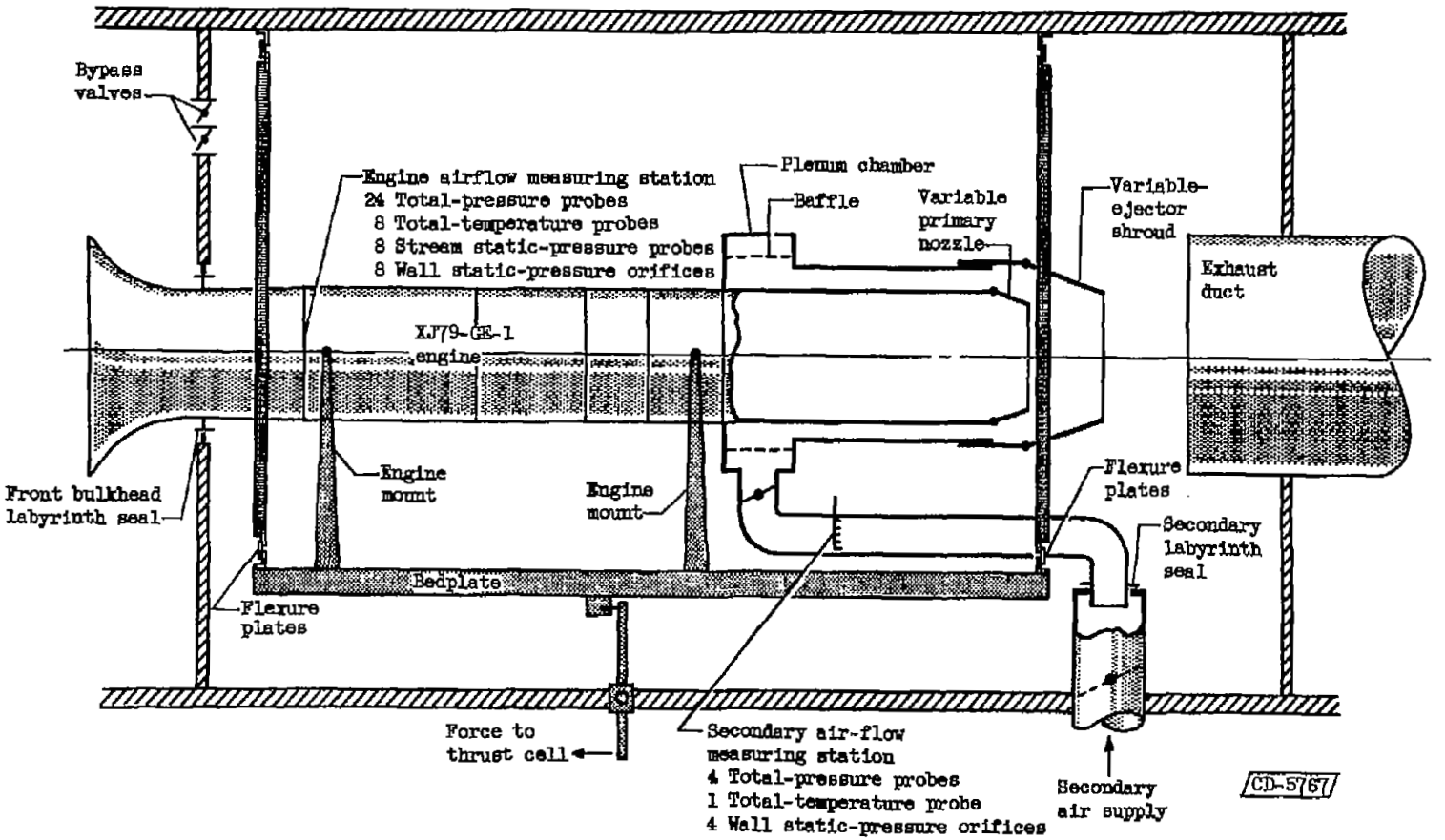

Figure 2. - Schematic drawing of test installation for XJ79-GE-1 engine installation.

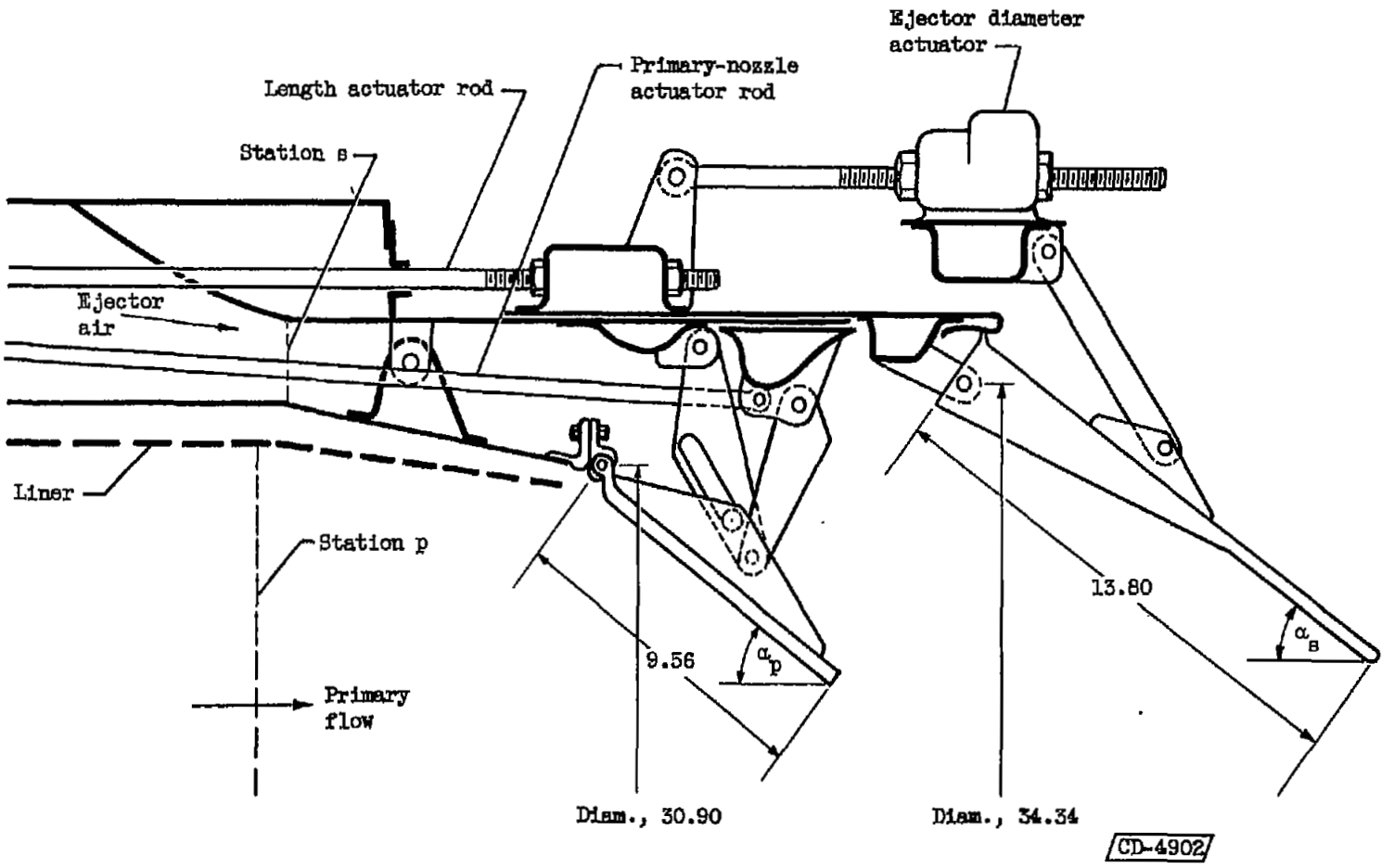

Figure 3. - Schematic diagram of XJ79-GE-1 variable-ejector assembly. (Dimensions are approximate and in inches.)

4630

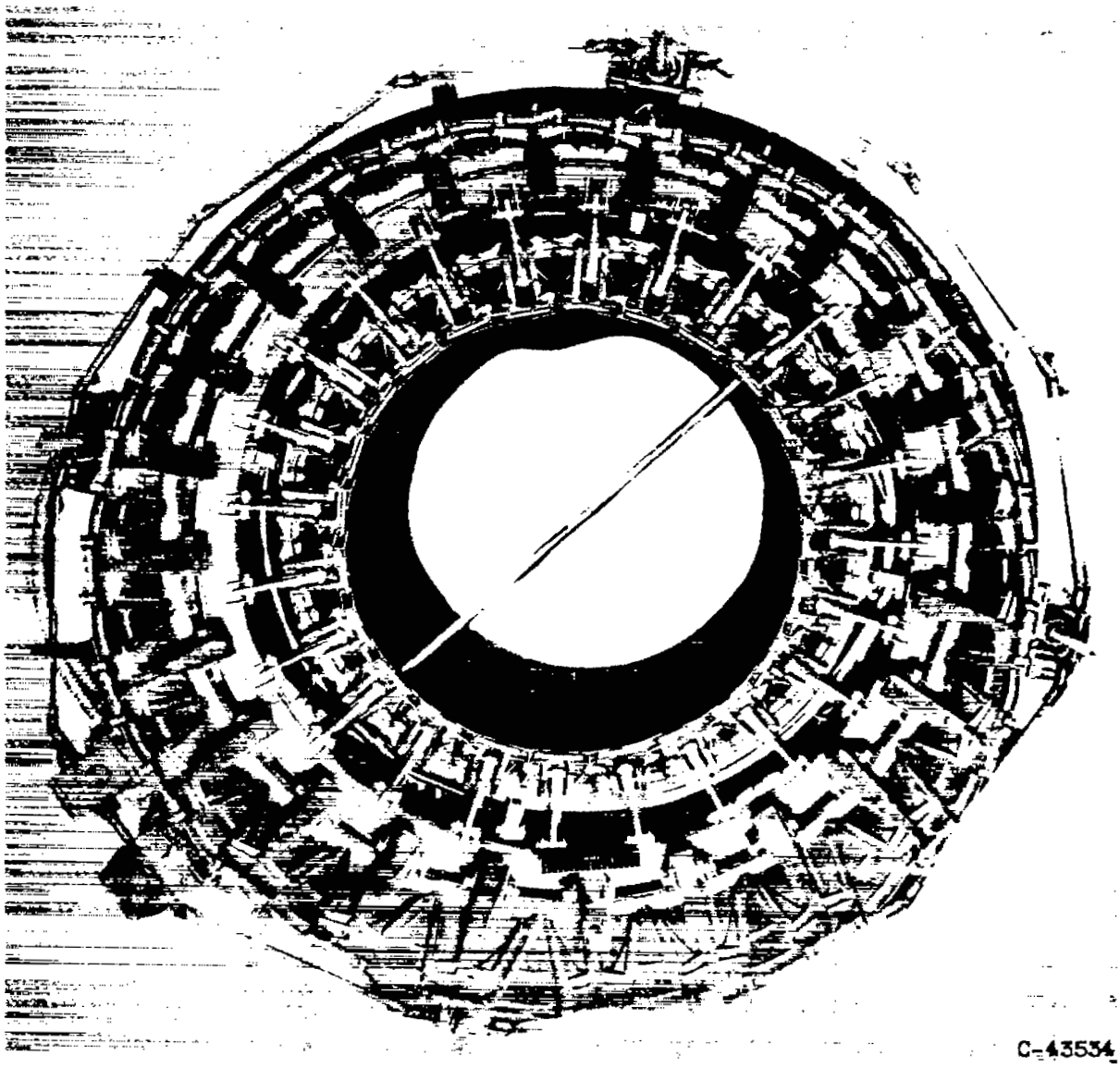

Figure 4. - XJ79-GE-1 variable primary nozzle with inside view of variable-ejector shroud.

4630

CI-3 back

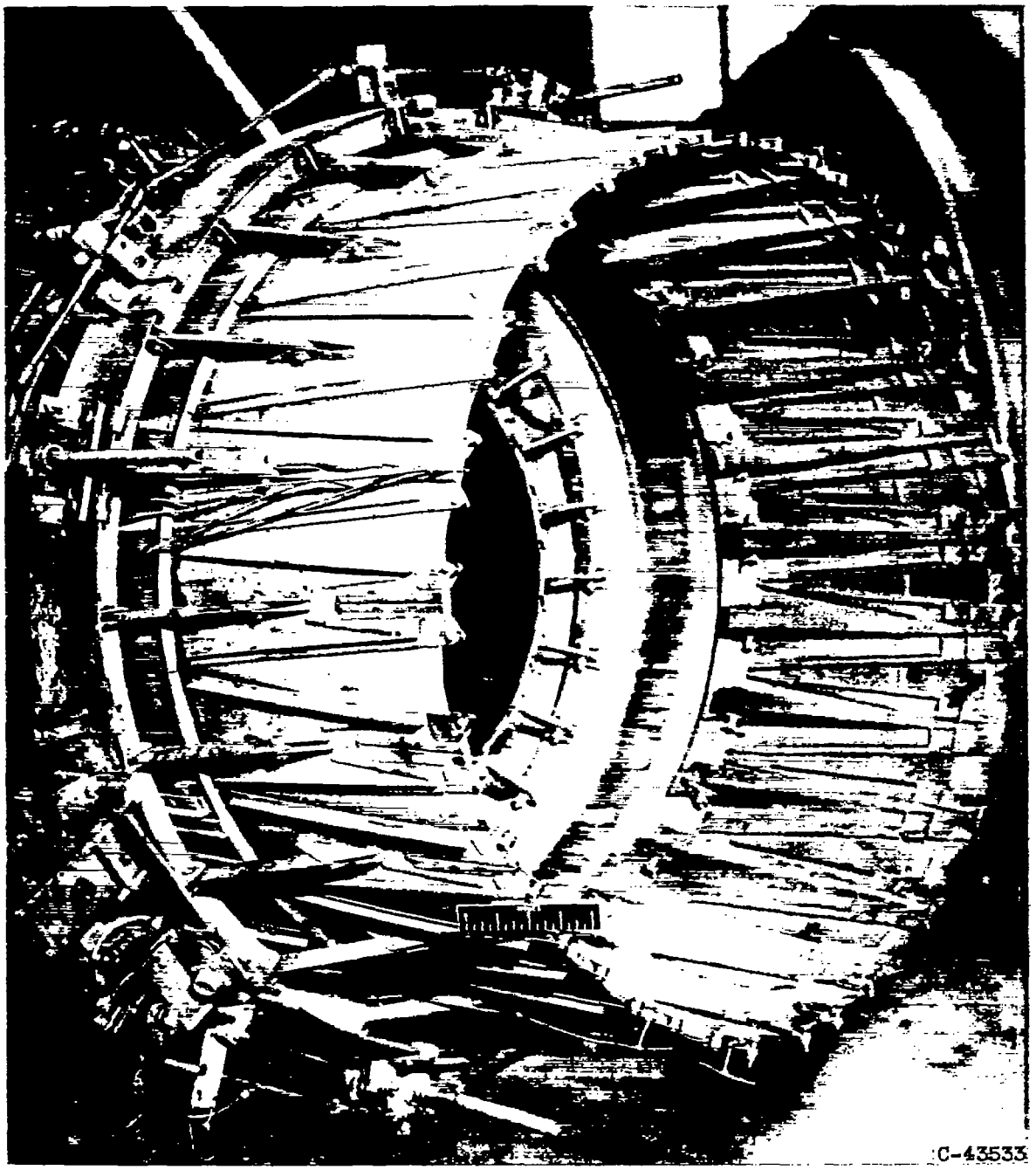

Figure 5. - View of XJ79-GE-1 variable-ejector shroud.

4630

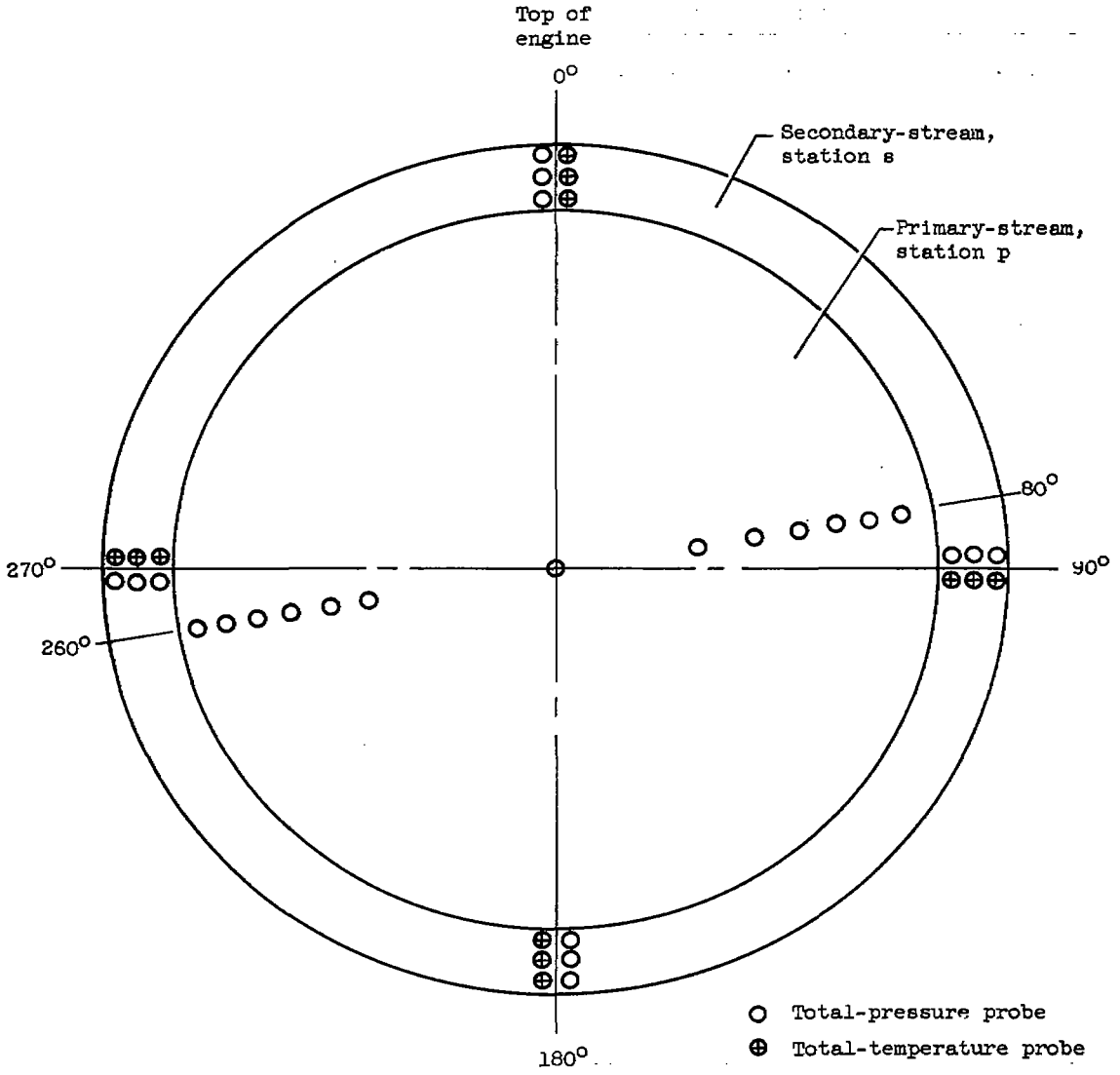

Figure 6. - Schematic diagram of basic ejector instrumentation, downstream view.

4630

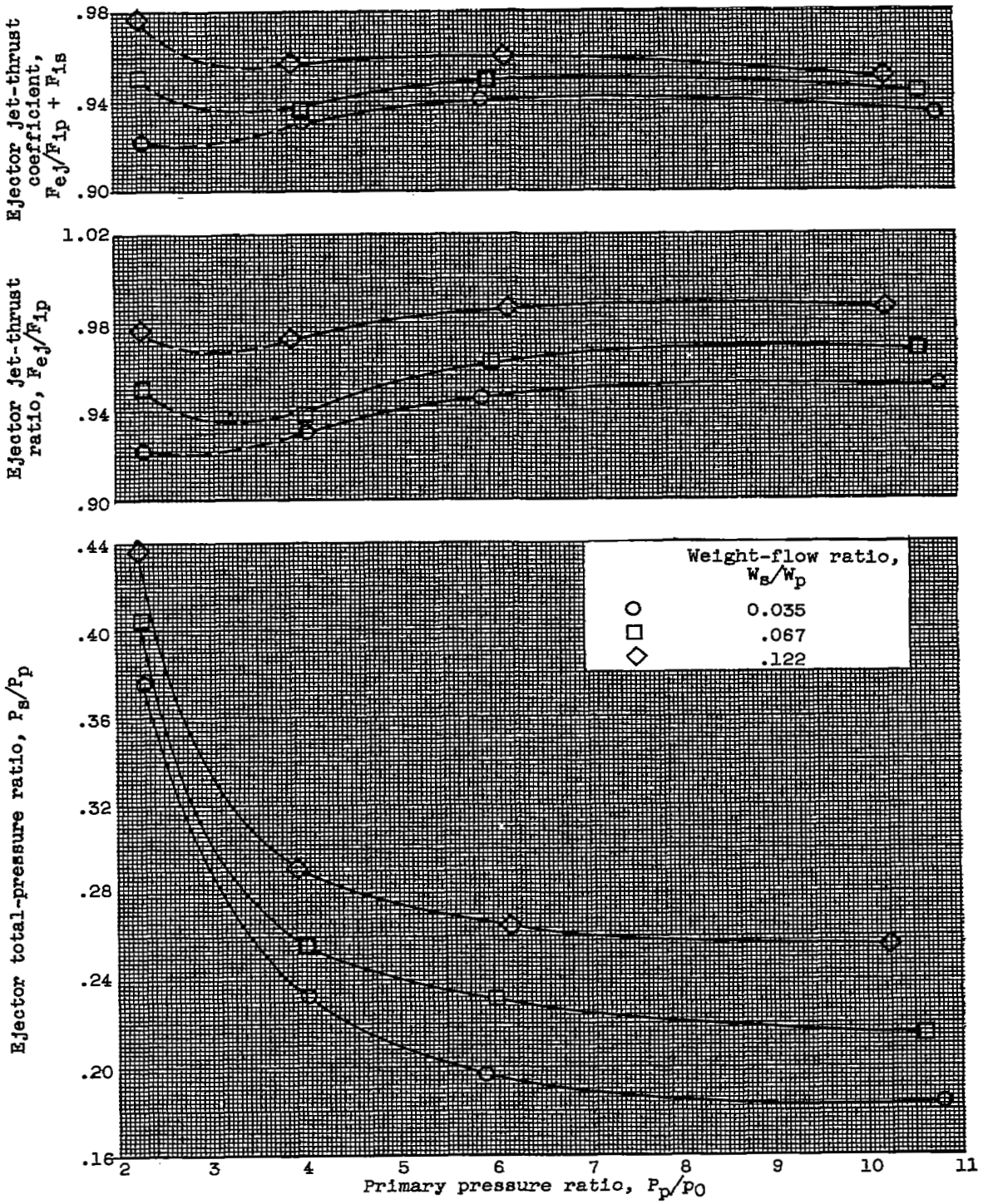

Figure 7. - Thrust and air-handling data for ejector configuration 1; D_p = 27.0 inches, D_e/D_p = 1.21, L/D_p = 0.78, and T_p = 2910° R.

4930

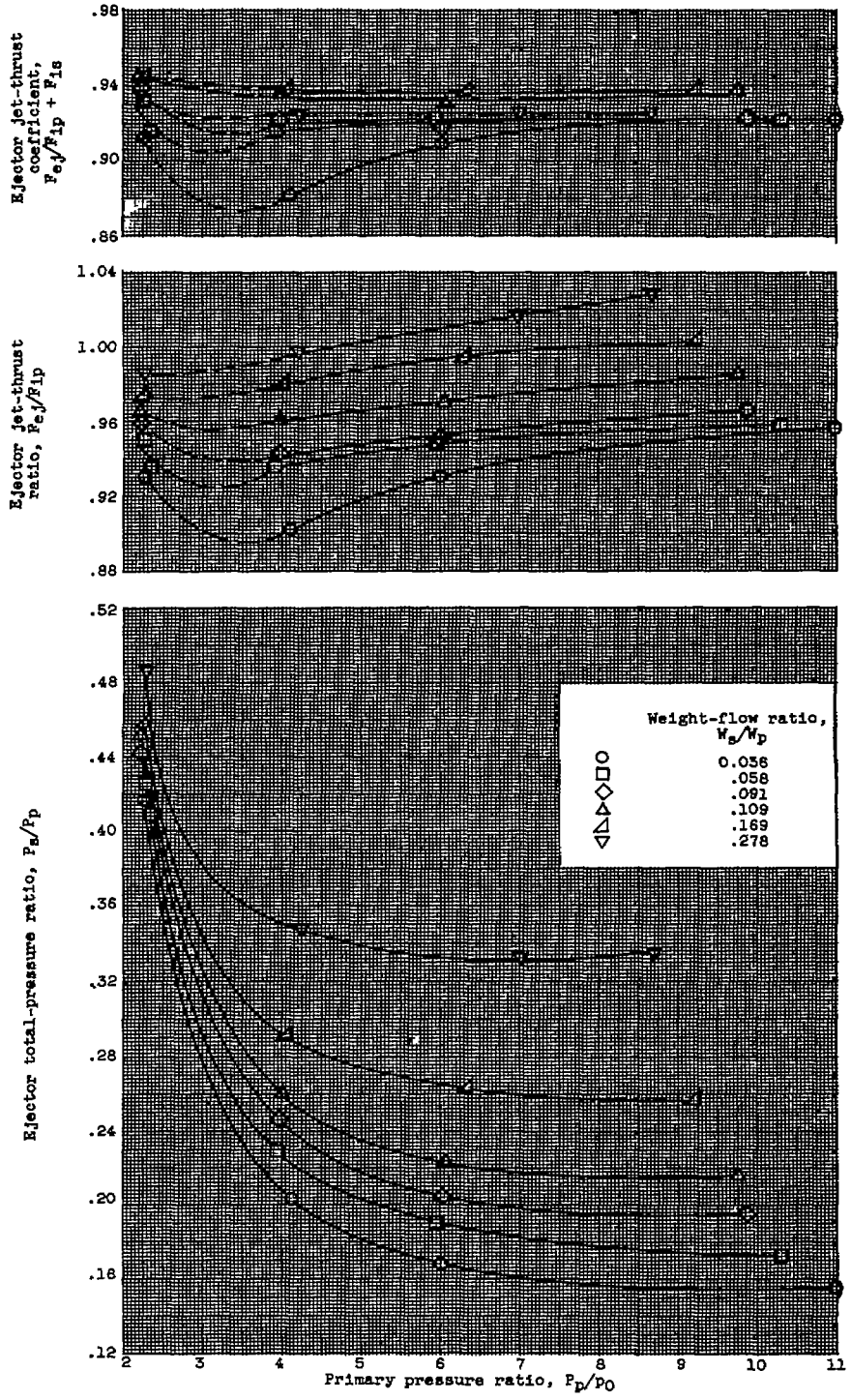

Figure 8. - Thrust and air-handling data for ejector configuration 2; D_p = 27.0 inches, D_e/D_p = 1.37, L/D_p = 0.78, and T_p = 2910° R.

4630

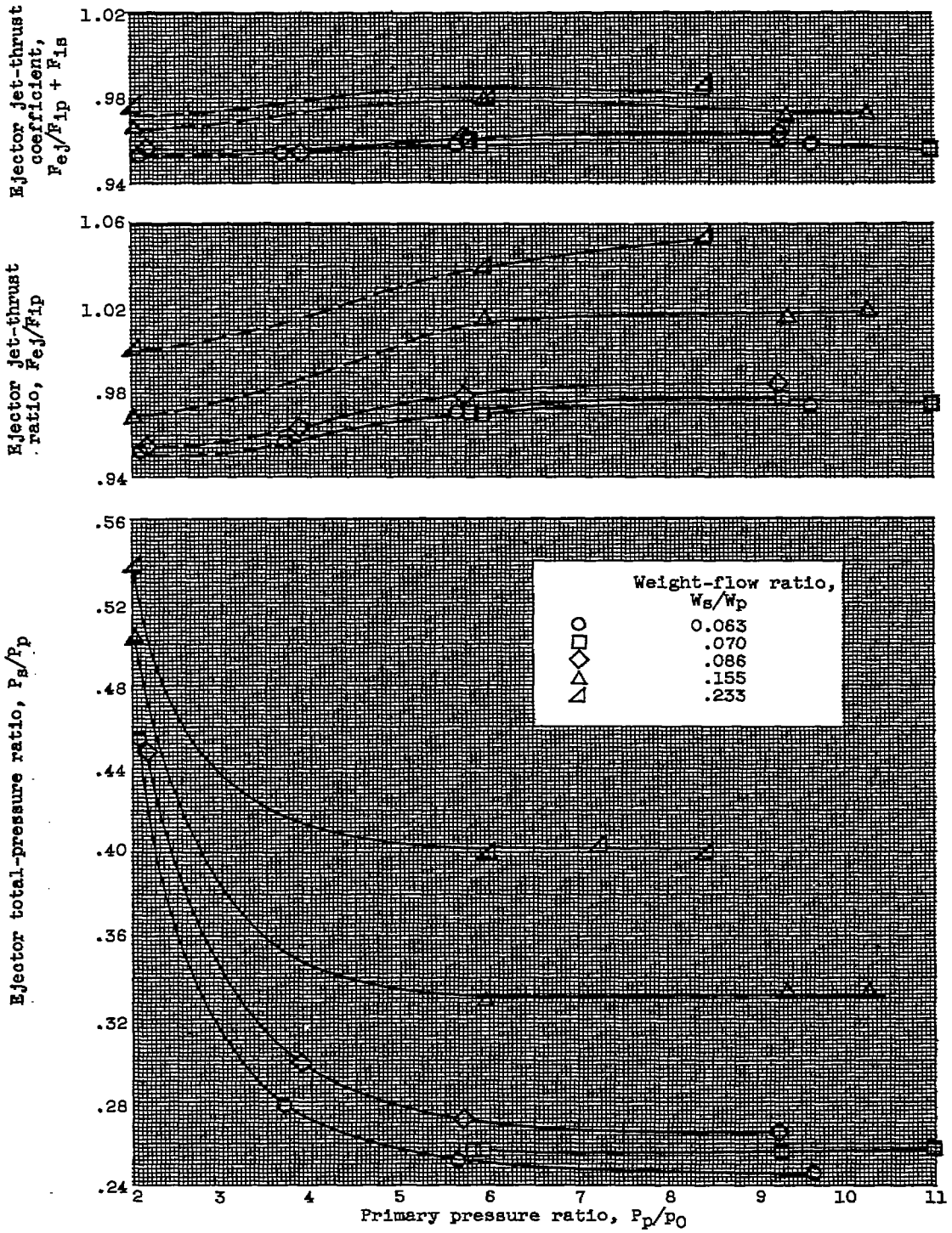

Figure 9. - Thrust and air-handling data for ejector configuration 3; D_p = 29.25 inches, D_e/D_p = 1.25, L/D_p = 0.71, and T_p = 3620° R.

4630

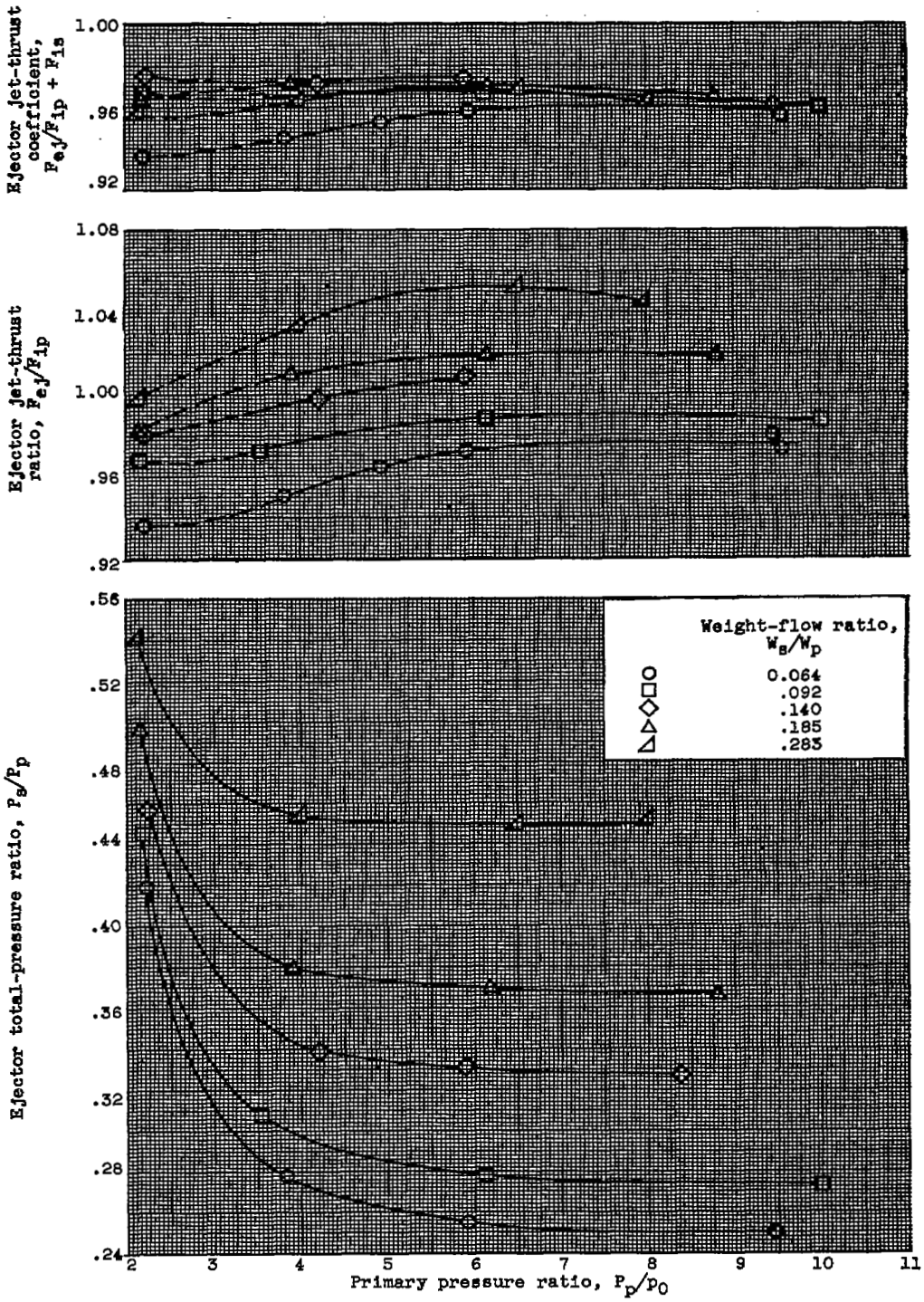

Figure 10. - Thrust and air-handling data for ejector configuration 4; D_p = 29.25 inches, D_e/D_p = 1.18, L/D_p = 0.71, and T_p = 3620° R.

4630

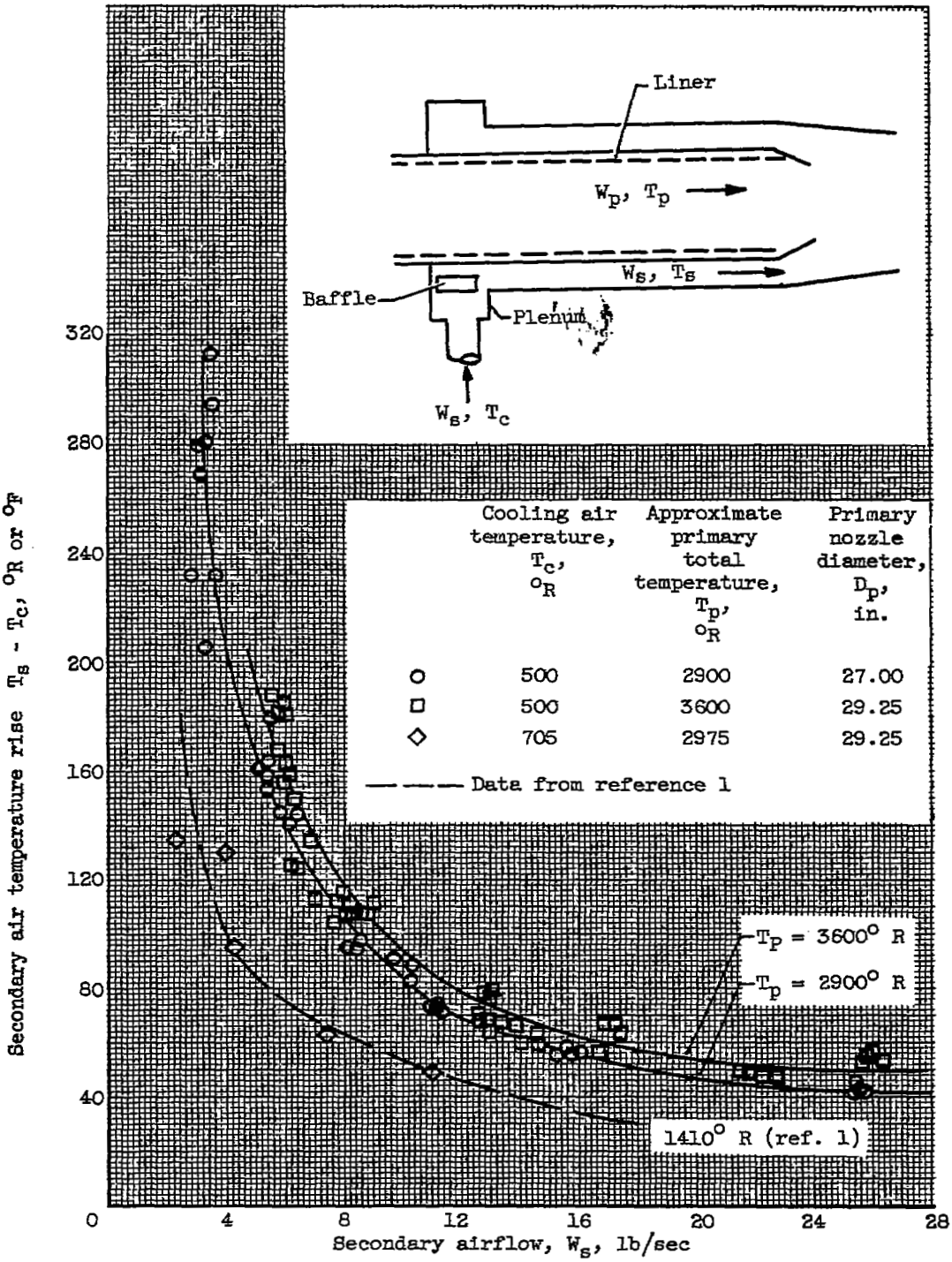

Figure 11. - Relation between secondary temperature rise and airflow.

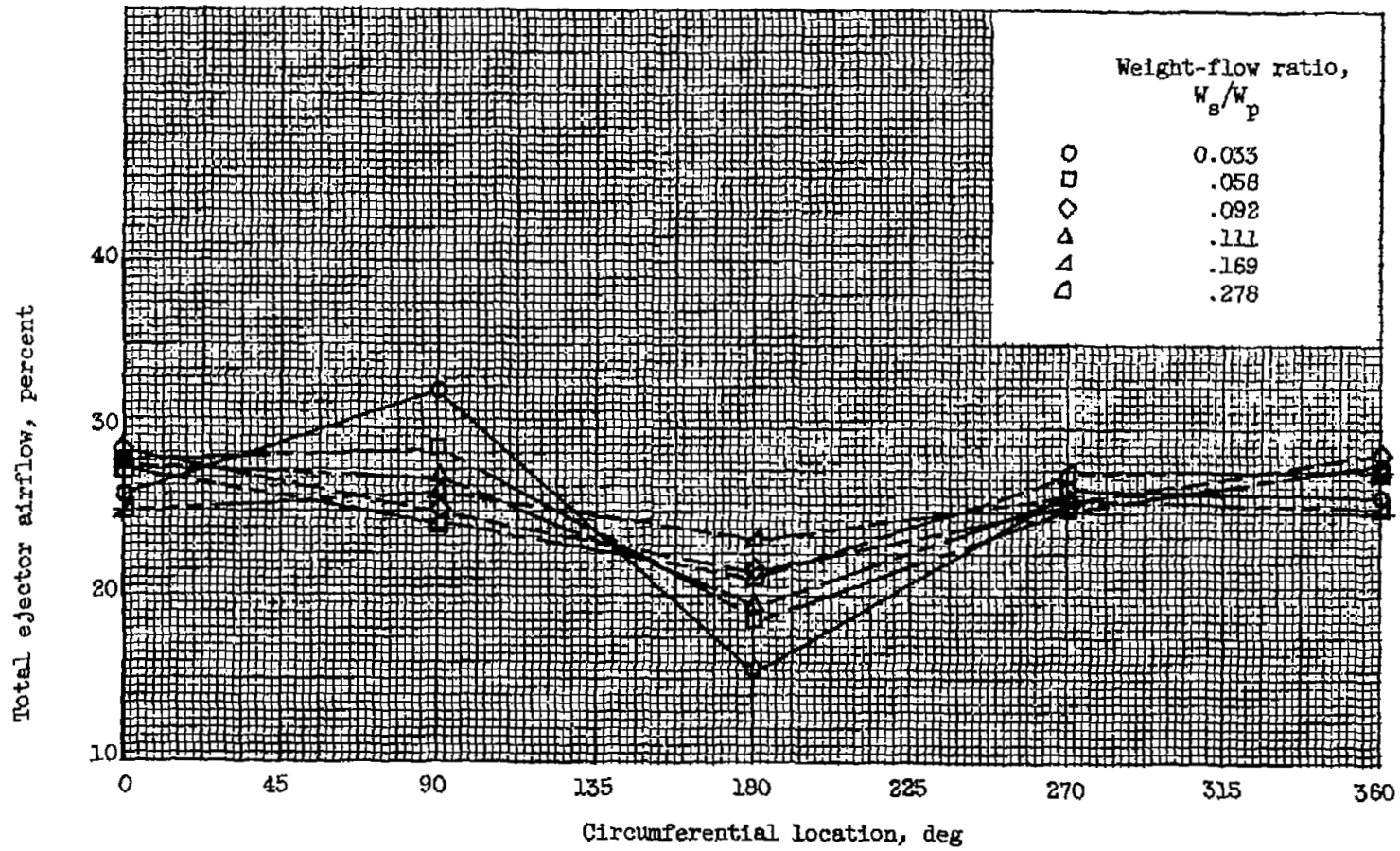

Figure 12. - Effect of weight-flow ratio on variation of mass distribution around shroud.

[redacted]

4630

PRELIMINARY INTERNAL PERFORMANCE DATA FOR A VARIABLE-EJECTOR ASSEMBLY ON THE XJ79-GE-1 TURBOJET ENGINE

II - AFTERBURNING CONFIGURATIONS

Harry E. Bloomer

Donald E. Groesbeck

Approved:

E. William Conrad
Chief
Engines Branch

Bruce T. Lundin
Chief
Propulsion Systems Division

atf - 6/26/57

[redacted]

LANGLEY RESEARCH CENTER
3 1176 01355 2501